THE JOURNAL OF BIOLOGICAL CHEMISTRY VOL. 289, NO. 12, pp. 8432–8441, March 21, 2014

Sustained High Protein-tyrosine Phosphatase 1B Activity in the Sperm of Obese Males Impairs the Sperm Acrosome Reaction*

Received for publication, September 17, 2013, and in revised form, January 30, 2014 Published, JBC Papers in Press, February 11, 2014, DOI 10.1074/jbc.M113.517466

Lei Shi[‡1], **Qipeng Zhang**[‡1], **Binqiang Xu**[§1], **Xiaohong Jiang**[‡], **Yutian Dai**[§2], **Chen-Yu Zhang**[‡3], **and Ke Zen**[‡4]

From the [‡]*Jiangsu Engineering Research Center for MicroRNA Biology and Biotechnology, State Key Laboratory of Pharmaceutical Biotechnology, School of Life Sciences, Nanjing University, Nanjing, Jiangsu 210093, China and the* [§]*Department of Urology, Affiliated Drum Tower Hospital, School of Medicine, Nanjing University, Nanjing, Jiangsu 210008, China*

Background: Obesity can cause male infertility or subfertility. The underlying mechanism, however, remains unclear.
Results: PTP1B level/activity in obese sperm are significantly higher than those in non-obese sperm. Sustained high PTP1B activity causes a prolonged NSF dephosphorylation, which impedes reassembly of the *trans*-SNARE complexes.
Conclusion: PTP1B serves as a link between male obesity and infertility/subfertility.
Significance: Identifying PTP1B as a novel therapeutic target in obesity-related male infertility/subfertility.

Evidence of a causal link between male obesity and subfertility or infertility has been demonstrated previously. However, the mechanism underlying this link is incompletely understood. Here, we report that sustained high protein-tyrosine phosphatase 1B (PTP1B) activity in sperm of obese donors plays an essential role in coupling male obesity and subfertility or infertility. First, PTP1B level and activity were significantly higher in sperm from *ob/ob* mice than in wild-type littermates. High PTP1B level and activity in sperm was also observed in obese patients compared with non-obese donors. The enhanced sperm PTP1B level and activity in *ob*/*ob* mice and obese patients correlated with a defect of the sperm acrosome reaction (AR). Second, treating sperm from male *ob*/*ob* mice or obese men with a specific PTP1B inhibitor largely restored the sperm AR. Finally, blockade of sperm AR by enhanced PTP1B activity in male *ob*/*ob* mice or obese men was due to prolonged dephosphorylation of *N*-ethylmaleimide-sensitive factor by PTP1B, leading to the inability to reassemble the *trans*-SNARE complexes, which is a critical step in sperm acrosomal exocytosis. In summary, our study demonstrates for the first time that a sustained high PTP1B level or activity in the sperm of obese donors causes a defect of sperm AR and that PTP1B is a novel potential therapeutic target for male infertility treatment.

The prevalence of overweight and obese individuals in the world's population has rendered these disorders the most difficult challenge to human health. Overweight and obesity impact not only cardiovascular diseases and diabetes but also many other disorders, such as male infertility (1). Recent population-based studies suggest an elevated risk of subfertility among couples in which the male partner is obese and an increased likelihood of abnormal semen parameters among heavier men (2). There is sound evidence that male obesity can be associated with reduced sperm concentrations, but studies addressing sperm motility, morphology, and DNA fragmentation have been contradictory. Although weight loss is the cornerstone of the treatment of obesity-related infertility, the mechanism underlying obesity and male infertility or subfertility is not completely understood.

The acrosome reaction (AR)[5] is a highly regulated membrane fusion process consisting of multiple stages that culminate in the attachment of secretory vesicles to the plasma membrane followed by the opening of fusion pores (3). Like other regulated exocytosis processes, the AR involves a large set of proteins. Previous studies have shown that exocytosis of sperm acrosome is dependent upon Rab3 activation and neurotoxin-sensitive soluble NSF attachment protein receptors (SNAREs) (4). Unlike other fusion scenarios where SNAREs are subjected to an assembly/disassembly cycle, the fusion machinery in sperm is regulated to ensure that SNAREs progress unidirectionally from a *cis* configuration in resting cells to monomeric and subsequently *trans* arrays in cells challenged with exocytosis inducers (5). In resting sperm, SNAREs are assembled in an inactive *cis* complex in the same membrane. At this stage, *N*-ethylmaleimide-sensitive factor (NSF) is phosphorylated on tyrosine. Upon activation, calcium derived from the extracellular medium activates RAS-associated protein RAB3A, triggering the tethering of the acrosome to the plasma membrane.

* This work was supported by National Basic Research Program of China Grants 2012CB517603 and 2011CB504803863; National Natural Science Foundation of China Grants 30988003, 30890044, 30800946, 30871019, 30890032, 31071232, 31100777, 31000323, 90608010, and 90813035; Research Fund for the Doctoral Program of Higher Education of China Grants 20100091120026 and 20100091120023; and Natural Science Foundation of Jiangsu Province Grant BK2011013.
[1] These authors contributed equally to this work.
[2] To whom correspondence may be addressed: Dept. of Urology, Nanjing Drum Tower Hospital, No. 321 Zhongshan Rd., Nanjing, Jiangsu 210008, China. E-mail: ytdai@hotmail.com.
[3] To whom correspondence may be addressed: JERC-MBB, School of Life Sciences, Nanjing University, Nanjing, Jiangsu 210093, China. Tel.: 86-25-84530247; E-mail: cyzhang@nju.edu.cn.
[4] To whom correspondence may be addressed: JERC-MBB, School of Life Sciences, Nanjing University, Nanjing, Jiangsu 210093, China. Tel.: 86-25-84530247; E-mail: kzen@nju.edu.cn.

[5] The abbreviations used are: AR, acrosome reaction; PTP, protein-tyrosine phosphatase; NSF, *N*-ethylmaleimide-sensitive factor; HTF, human tubal fluid; TeTx, tetanus toxin; CTC, chlortetracycline fluorescence; IVF, *in vitro* fertilization; SNAP, soluble NSF attachment protein.

Tethering initiates the activation and/or recruitment of protein-tyrosine kinases and phosphatases (PTPs) to the membrane fusion sites. Then PTPs dephosphorylate NSF (6, 7). Once dephosphorylated, NSF, together with α-synaptosome-associated protein (α-SNAP), disassembles *cis*-SNARE complexes. At the final stage that is triggered by an efflux of calcium from the intra-acrosomal store, monomeric SNAREs are reassembled in tight *trans*-complexes and promote the fusion between acrosome membranes and sperm surface membranes (6, 8, 9). In this model, the dynamic process of NSF dephosphorylation by PTPs plays a key role in controlling the disassembly or reassembly of *cis*-SNARE or *trans*-SNARE complexes.

Protein-tyrosine phosphatase 1B (PTP1B) is the prototype of the superfamily of PTPs and belongs to the non-transmembrane subfamily 1 of intracellular PTPs (10, 11). PTP1B is an abundant enzyme that is expressed in all insulin-responsive tissues, including skeletal muscle, liver, adipose tissue, and brain (12, 13), where it is localized predominantly on intracellular membranes by a hydrophobic C-terminal targeting sequence. PTP1B has been implicated in the negative regulation of insulin and leptin signaling (14, 15). In a recent excellent study by Zarelli *et al.* (6), PTP1B was shown to dephosphorylate NSF and elicit SNARE complex disassembly during human sperm exocytosis, suggesting that NSF is a substrate of PTP1B and that PTP1B may play a critical role in controlling sperm AR.

In the present study, we determined the expression level and activity of PTP1B in sperm under various conditions and the role of PTP1B in modulating the sperm AR. Our results confirm that obese males generally have a sustained high PTP1B level and activity, which can impair the reassembly of SNAREs into *trans*-SNAREs complexes and cause a defect of the sperm AR. Because the PTP1B-specific inhibitor can largely restore the sperm AR in *ob*/*ob* mice and obese men, our study also presents PTP1B as a novel therapeutic target in male infertility treatment.

EXPERIMENTAL PROCEDURES

Human and Mouse Samples—This study was approved by the Hospital Ethical Examination Committee of Human Research of Nanjing Drum Tower Hospital, Nanjing University (Nanjing, China), and written informed consent was obtained from each participant. Human semen samples were used in this study after routine semen analysis. Age and body mass index were recorded for all sperm donors. The donors were divided into two groups: 28 obese or overweight (body mass index > 25) and subfertile/infertile men with a normal proportion of intact acrosome and 28 age-matched healthy donors. Semen was allowed to liquefy for 30 – 60 min at 37 °C. Following a swim-up protocol to isolate highly motile cells, sperm concentrations were adjusted to 7×10^6/ml before incubating in culture media (human tubal fluid (HTF) medium (Irvine Scientific, Santa Ana, CA)). For the fertility study in obese mice, we used 10-week old *ob*/*ob* (C57BL/6J background) and C57BL/6J (WT) male mice obtained from the Model Animal Research Center of Nanjing University (Nanjing, China). For mouse samples, spermatozoa from caudae epididymides and vasa deferentia were released into PBS or HTF medium. Animal maintenance and experimental procedures were carried out in accordance with the United States National Institute of Health Guidelines for the Use of Experimental Animals and approved by the Animal Care Committee of Nanjing University (Nanjing, China).

PTP1B Inhibitor Treatment and Induction of AR—After a swim-up, the sperm cells were incubated for at least 120 min under conditions that support capacitation (HTF, 37 °C, 5% CO_2, 95% air). The capacitated spermatozoa were pretreated with a specific PTP1B inhibitor FRJ (3-(3,5-dibromo-4-hydroxy-benzoyl)-2-ethyl-benzofuran-6-sulfonic acid) (Santa Cruz Biotechnology, Inc.) or DMSO (0.1%) as a control for 10 min at 37 °C to prevent PTP1B activity, followed by 2 μM tetanus toxin (TeTx) (4) from *Clostridium tetani* and 15 μM progesterone (16) (both from Sigma) treatment for an additional 10 min. Spermatozoa suspensions were then collected for CTC staining, Western blot analysis, and indirect immunofluorescence.

Chlortetracycline Fluorescence (CTC) Assay—Spermatozoa were stained with CTC essentially as described previously (17). The stain solution, containing 750 μM CTC (Sigma) in a buffer containing 130 mM NaCl, 5 mM L-cysteine, 20 mM Tris-HCl (pH 7.8), was prepared daily and stored at 4 °C in the dark. A 10-μl sample of sperm suspension was mixed with 10 μl of CTC stock solution in a 200-μl Eppendorf tube at room temperature. Then 5 μl of 12.5% glutaraldehyde in 2 M Tris buffer (pH 7.8) was added as a fixative and was thoroughly mixed with the sample. The samples were kept at 37 °C for 1 h. Slides were prepared by placing 10 μl of the suspension onto a clean microscope slide. A drop of antifade solution (Invitrogen) was mixed in carefully to delay the fading of the fluorescence. A coverslip was placed on top, and the slide was gently but firmly compressed between two tissues. Any excess fluid was removed, and the number of spermatozoa lying flat on the slide was maximized; their flat orientation was crucial for accurate assessment. The acrosome-intact pattern represents capacitated but acrosome-intact sperm, and the acrosome-reacted pattern corresponds to sperm that underwent both capacitation and AR. A total of 200 spermatozoa from seven independent experiments were analyzed to calculate the AR rate.

Protein Extraction and Western Blot Analysis—Proteins were extracted in sample extraction buffer (50 mM Tris, 150 mM NaCl, 1% Triton X-100, 0.1% SDS, 1 mM PMSF, 25 mM β-glycerophosphate, 1 mM Na_3VO_4, 2 μg/ml leupeptin, and 2 μg/ml aprotinin, pH 7.4), and the protein concentration was determined using a BCA kit (Thermo, Billerica, MA). Equal amounts of protein samples were separated by electrophoresis on 12% SDS-polyacrylamide gels and transferred to PVDF membranes. The membranes were blocked in TBST (50 mM Tris, 150 mM NaCl, 0.05% Tween 20, pH 7.6) containing 5% nonfat dry milk or BSA and immunoblotted with rabbit monoclonal anti-PTP1B (1:2000; Abcam, Cambridge, MA), rabbit polyclonal anti-VAMP2 (1:1000; Abcam), mouse monoclonal anti-phosphotyrosine (P-Tyr-100) (1:1000; Cell Signaling, Danvers, MA), rabbit monoclonal anti-NSF (1:1000; Cell Signaling), and mouse monoclonal anti-GAPDH (1:3000; Santa Cruz Biotechnology). Horseradish peroxidase-conjugated goat-anti-mouse IgG or goat-anti-rabbit IgG was used as secondary antibody (1:3000; Santa Cruz) with 1-h incubations. Protein bands were visualized with enhanced chemiluminescence and quantified by densitometry using ImageJ.

Immunoprecipitation—For the immunoprecipitation assay, the cells were lysed with lysis buffer. Overall, 200 μg of whole-

cell lysates were incubated with protein-specific antibodies overnight at 4 °C, followed by precipitation of the antibody-protein complex using Protein G-agarose beads (Santa Cruz Biotechnology). In each immunoprecipitation experiment, an isotype negative control was used. After washing with lysis buffer, precipitates were analyzed for phospho-NSF or PTP1B by Western blot and were dissolved in 100 μl of diethanolamine to continue to test PTP1B activity at the mean time.

Protein-tyrosine Phosphatase 1B Activity Measurement—PTP1B activity was measured using the phosphatase substrate kit (Thermo Scientific, Waltham, MA) following the manufacturer's instructions. To each well of the 96-well plate was added 10 mM *p*-nitrophenyl phosphate (*p*-NPP) and 50 μl of PTP1B solution with or without test compounds (final volume 100 μl). Following a 30-min incubation period at room temperature, the reaction was terminated with 50 μl of 2 M NaOH. The amount of *p*-nitrophenol produced was estimated by measuring the absorbance at 405 nm.

Indirect Immunofluorescence and Double-labeled Fluorescence—Sperm samples were smeared onto slides, fixed with 4% paraformaldehyde in PBS for 15 min at room temperature, permeabilized with 0.1% Triton X-100 in PBS for 20 min, and blocked with goat serum for 30 min at room temperature. Mouse monoclonal anti-SNAP25 (1:100; Abcam) and rabbit polyclonal anti-VAMP2 (1:100; Abcam) or rabbit monoclonal anti-PTP1B (1:100; Abcam) and mouse monoclonal anti-NSF (1:100; Abcam) were diluted in 5% goat serum in PBS, added to the slides, and incubated overnight at 4 °C in a humidified chamber. Spermatozoa were incubated with Alexa Fluor546-conjugated goat anti-rabbit IgG and Alexa Fluor488-conjugated goat anti-mouse IgG (Invitrogen) at a dilution of 1:100 for 1 h at room temperature and were observed by fluorescence microscopy at excitation wavelengths of 488 and 546 nm.

In Vitro Fertilization (IVF)—Eggs were surgically removed from female 3–4-week-old WT mice. Three days prior to the scheduled IVF procedure, 5 IU of pregnant mare serum gonadotropin (Sigma) was intraperitoneally injected into the egg donor mice. 46–48 h after the pregnant mare serum gonadotropin injection, 5 IU of human chorionic gonadotropin (Sigma) was intraperitoneally injected into the same egg donor mice. Cumulus-oocyte complexes were placed into HTF medium with capacitated sperm and incubated at 37 °C in a humidified atmosphere of 5% CO_2 and 95% air. The sperm were washed away after 4–6 h, and the eggs were cultured overnight in an incubator. Using a stereomicroscope, the fertilization was calculated by counting the number of embryos that have reached the 2-cell stage of development and the total number of eggs. The 2-cell embryos correspond to successful fertilization and sperm cells that underwent both capacitation and AR. A total of 100 embryos from seven independent experiments were analyzed to calculate the fertilization rate.

Statistical Analysis—All images of Western blot assays are representative of at least three independent experiments. To assess the possible effects of the PTP1B inhibitor, we calculated the percentage of sperm with B and AR CTC staining patterns. AR indexes were calculated by subtracting the number of spontaneously reacted spermatozoa from all values and expressing the results as a percentage of the AR observed in the positive control. Data were evaluated using one-way analysis of variance. The data are presented as means ± S.D. from at least three independent experiments. The Tukey-Kramer post hoc test was used for pairwise comparisons. Differences were assessed using the Wilcoxon rank sum (Mann-Whitney) test for unpaired samples. p values <0.05 were considered significant.

RESULTS

Normal Level of PTP1B Is Required for AR in Mouse Spermatozoa—The up-regulation of PTP1B has been reported in various tissues of obese, diabetic, or insulin-resistant animal models and patients, including skeletal muscle, adipose tissue, and liver (18–24). To determine whether the up-regulation of PTP1B expression also occurs in spermatozoa under obese conditions, we examined PTP1B protein expression levels and activities in *ob*/*ob* mice and their WT littermates. In this experiment, spermatozoa were incubated in HTF medium at 37 °C in 5% CO_2 for 120 min for capacitation and then collected for Western blot analysis. As shown in Fig. 1, the PTP1B protein level in the spermatozoa of *ob/ob* mice was significantly higher (about 3-fold) than in WT mice (Fig. 1, *A* and *B*), which is in agreement with previous studies demonstrating up-regulation of PTP1B in other tissues of *ob*/*ob* mice (25, 26). Because increased PTP1B expression generally correlates with increased PTP1B activity (18, 19, 23), we also examined the activity of PTP1B in the spermatozoa of *ob*/*ob* mice and their WT littermates and observed that PTP1B activity was significantly higher in the spermatozoa of *ob*/*ob* mice than in control WT mice (Fig. 1*C*). Interestingly, the enhanced activity of PTP1B in the spermatozoa of *ob*/*ob* mice was dose-dependently decreased by a PTP1B-specific inhibitor (FRJ). Previous studies suggested that this compound modulates PTP1B activity by binding to a novel binding site that is distal to the active site of PTP1B, named the WPD loop (27). As observed in Fig. 1*C*, the IC_{50} of this PTP1B inhibitor was 8.0 μM.

We next examined the effect of PTP1B on the AR of mouse sperm. Briefly, the capacitated spermatozoa were incubated under different conditions with or without 12 μM PTP1B inhibitor, and progesterone was introduced to initiate the sperm AR. Spermatozoa suspensions were then collected for evaluation of the AR by CTC staining. As shown in Fig. 1, *D* and *E*, the AR rate of *ob*/*ob* mouse spermatozoa was significantly lower than that of control spermatozoa. However, this impairment of AR in *ob*/*ob* mouse spermatozoa could be largely restored after treating spermatozoa with the PTP1B inhibitor.

The IVF assay was then performed to test whether controlling PTP1B activity by a chemical inhibitor could restore fertilization in *ob/ob* mice (Fig. 1, *F* and *G*). Similar to the result of the AR rate, *ob/ob* mouse spermatozoa failed in fertilization, but this defect of fertilization was largely restored by inhibiting PTP1B activity using PTP1B inhibitor. These results suggest that PTP1B is a potential molecular target of male infertility or subfertility due to obesity.

Sustained High PTP1B Activity in ob/ob Mouse Spermatozoa Impairs SNARE Complex Reassembly via NSF Dephosphorylation—NSF plays a key role in controlling the disassembly and reassembly cycle of the SNARE complex, an essential component of the membrane fusion machinery. As a substrate

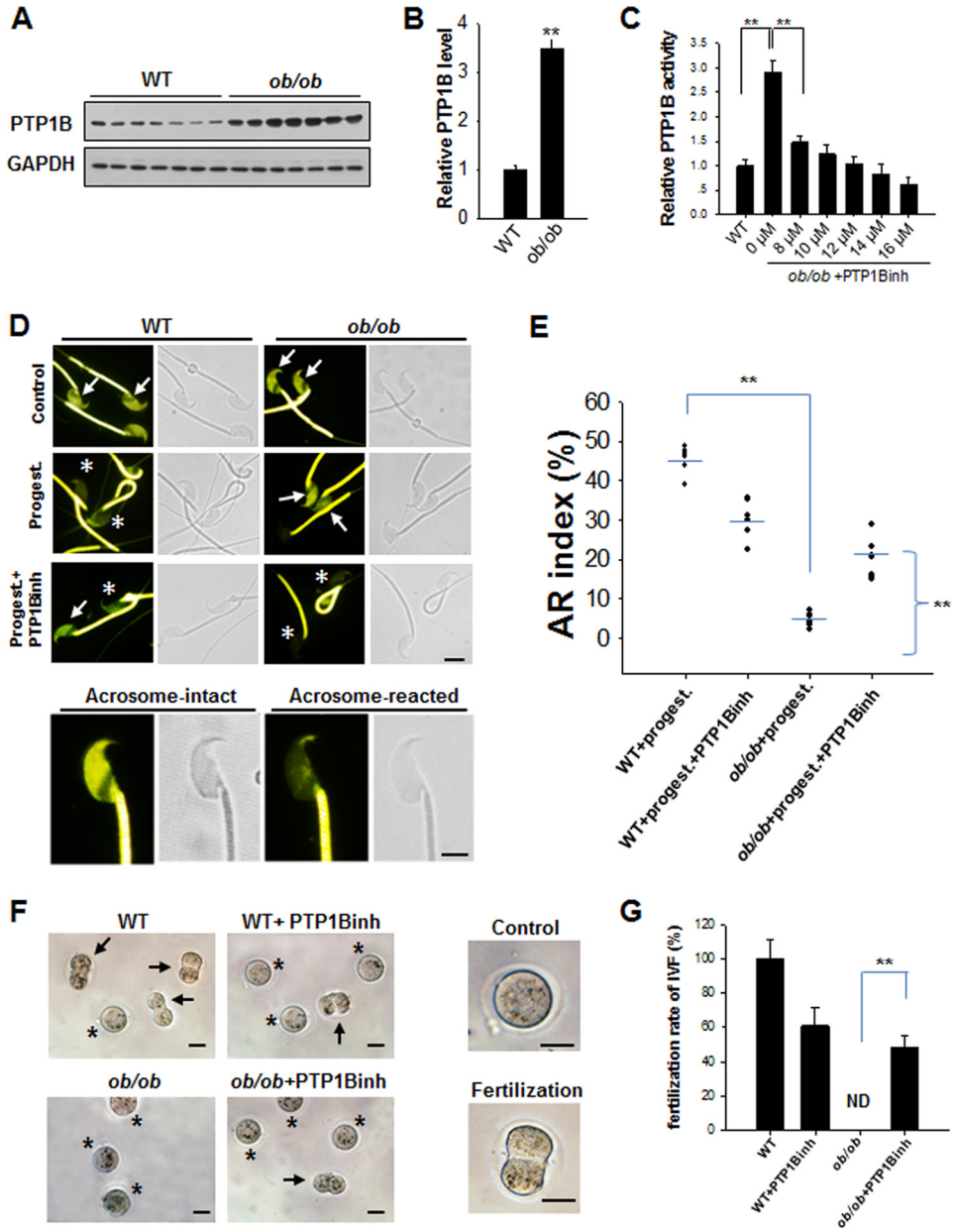

FIGURE 1. **The spermatozoa of *ob/ob* mice process a sustained high expression level and activity of PTP1B.** *A*, PTP1B protein levels in spermatozoa of WT and *ob/ob* mice were determined by Western blot. *B*, quantitative analysis of Western blot results. **, $p < 0.01$. *C*, dose-dependent inhibition of PTP1B activity in *ob/ob* mouse spermatozoa by PTP1B inhibitor (*PTP1Binh*). $n = 7$. **, $p < 0.01$. *D*, CTC staining of WT and *ob/ob* mouse sperm. Spermatozoa from WT and *ob/ob* mice were stained by CTC and fixed by glutaraldehyde. By CTC staining, two different patterns of sperm were detected on the sperm head: acrosome-intact sperm (*arrows*) and Acrosome-reacted sperm (*asterisks*). All sperm present strong labeling in the principal piece of the flagellum. *Scale bar*, 3 μm. *E*, quantitative analysis of CTC staining of the sperm AR. A total of 200 spermatozoa from seven independent experiments were divided into two patterns (shown above) to be analyzed. *F*, IVF assay using spermatozoa treated with or without PTP1B inhibitor. Two patterns were detected, control (*asterisks*) and fertilization (2-cell) embryos (*arrows*). *G*, quantitative analysis of IVF results. A total of 100 embryos from seven independent experiments were divided into two patterns (shown above) to calculate the fertilization rate. **, $p < 0.01$. *Scale bar*, 50 μm. *Error bars*, S.D.

of PTP1B, NSF can be dephosphorylated by PTP1B, and dephosphorylated NSF would cause the disassembly of *cis*-SNARE complexes (6). To confirm the link between PTP1B and NSF, we detected the location of NSF and PTP1B in spermatozoa from *ob/ob* mice and WT mice. As shown in Fig. 2*A*, NSF was labeled in the sperm acrosomal region after capacitation, whereas PTP1B was localized to the equatorial segment of *ob*/*ob* mice and WT sperm. Following progesterone stimulation, a part of PTP1B was co-localized with NSF in the sperm acrosomal region. Our results indicate that PTP1B and NSF still respectively locate in different regions of sperm cells before progesterone stimulation, although PTP1B remains a sustained higher level in spermatozoa of *ob/ob* mice. Then we examined the level of tyrosine-phosphorylated NSF in spermatozoa from *ob*/*ob* mice and WT mice (Fig. 2*B*). As can be seen, there is no difference in the level of phosphorylated NSF between WT mice sperm and *ob/ob* mouse sperm at resting status (without stimulation with progesterone). Progesterone stimulation induced a dramatic dephosphorylation of NSF. Notably, PTP1B inhibitor alone had no effect on phosphorylation of NSF at rest-

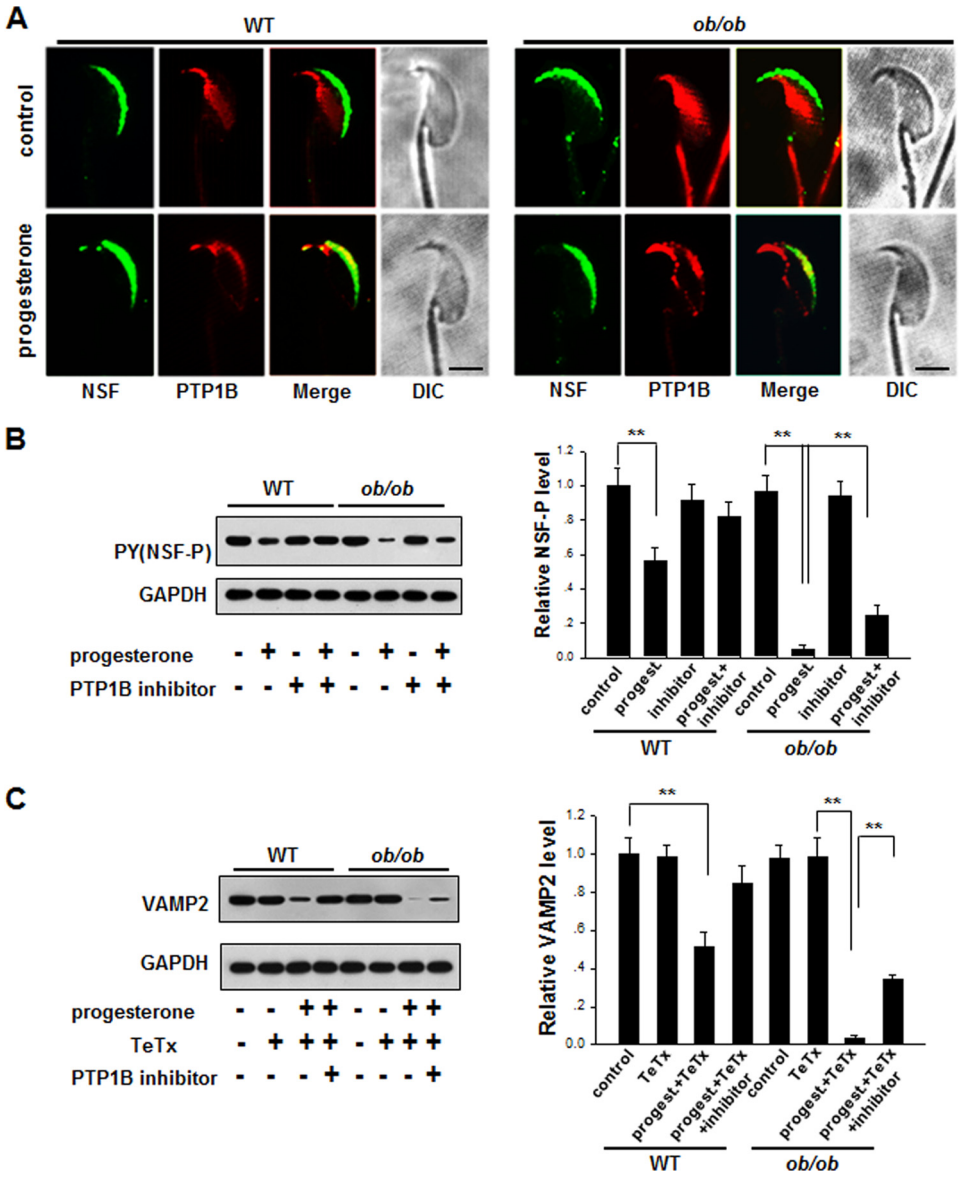

FIGURE 2. **Sustained high PTP1B activity in *ob*/*ob* mouse spermatozoa results in a prolonged dephosphorylation of NSF and defect in the formation of VAMP2 complexes stimulated by progesterone.** *A*, immunofluorescence staining of PTP1B and NSF in sperm with or without progesterone stimulation. *Scale bar*, 3 μm. *B*, the level of phosphorylated NSF (*pY*, *NSF-P*) in the spermatozoa of WT and *ob/ob* mice that were incubated in HTF medium (37 °C, 120 min) with or without PTP1B inhibitor for capacitation. *C*, the level of VAMP2 sensitive to TeTx-induced proteolytic cleavage in the presence or absence of PTP1B inhibitor. The capacitated spermatozoa of WT and *ob/ob* mice were pretreated with PTP1B inhibitor for 10 min, followed by progesterone (*progest*) for 10 min. **, $p < 0.01$, $n = 7$. *Error bars*, S.D.

ing status, which is consistent with our observation that PTP1B did not co-locate with NSF before progesterone stimulation. However, compared with WT mice, ob/ob mice had a significantly lower level of tyrosine-phosphorylated NSF in sperm when the sperm were activated by progesterone. This result is in agreement with the observation that *ob*/*ob* mouse sperm contain higher PTP1B activity than WT mouse sperm (Fig. 1), and the high PTP1B activity results in NSF dephosphorylation after progesterone stimulation. As expected, the level of tyrosine-phosphorylated NSF in spermatozoa from *ob/ob* mice was reversed after inhibiting PTP1B activity in sperm by PTP1B inhibitor.

Based on the observation that high PTP1B activity induces a lower level of NSF tyrosine phosphorylation in sperm after progesterone stimulation, we then analyzed the dynamics of SNARE assembly and disassembly during the sperm AR. Briefly, we treated mouse sperm with various reagents, including a PTP1B inhibitor and progesterone, and incubated the sperm with the clostridial neurotoxin, TeTx, for 10 min. Previous studies have shown that monomeric SNAREs can be cleaved by TeTx, whereas SNAREs engaged in loose (partially assembled at their N-terminal portions) *trans* complexes (4, 28, 29) or *cis* complexes are resistant to TeTx (30). Therefore, detecting the level and location of SNARE components after TeTx cleavage can provide information about the disassembly and reassembly of SNARE complexes. As shown by Western blot analysis in Fig. 2*C*, when TeTx was introduced, the level of synaptobrevin (VAMP2) was decreased in sperm from both control WT and *ob*/*ob* mice after progesterone stimulation, indicating that progesterone stimulation disrupted the *cis*-

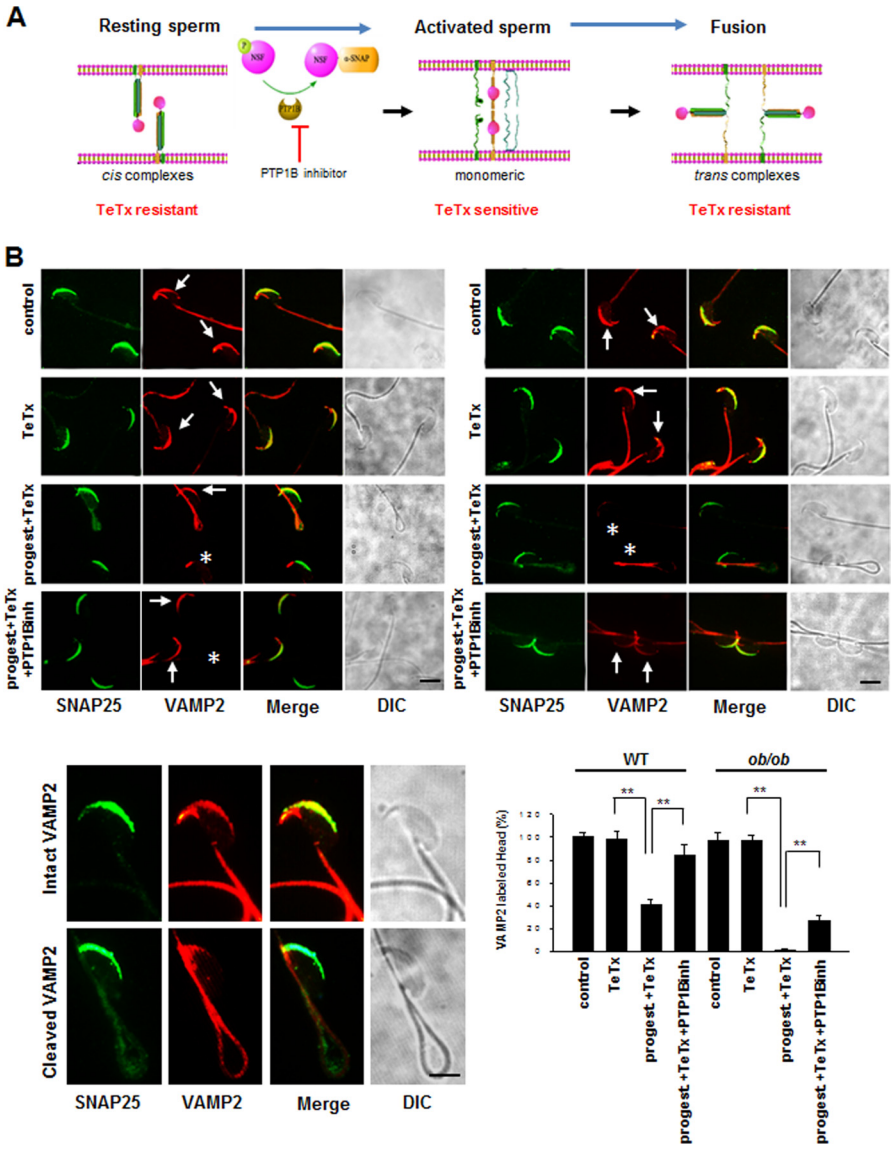

FIGURE 3. **Sustained high PTP1B activity in *ob/ob* mouse spermatozoa impairs the SNARE complex reassembly under the stimulation with progesterone.** *A*, schematic illustration of *cis*-SNARE complex disassembly and the reassembly of *trans*-SNARE complexes in sperm during the AR. *B*, double staining of VAMP2 (sensitive to TeTx) and SNAP25 (resistant to TeTx) in capacitated spermatozoa of WT and *ob/ob* mice after treatment with or without the combination of PTP1B inhibitor, TeTx, or progesterone for 10 min. *Asterisks* indicate the cells in which the VAMP2 immunostaining signals at acrosomal region are absent. *Arrows* indicate the cells that have intact VAMP2 immunostaining signals at the acrosomal region. *DIC*, differential interference contrast. **, $p < 0.01$, $n = 5$; a total of about 200 spermatozoa heads were counted to calculate two above patterns. *Scale bar*, 3 μm. *Error bars*, S.D.

SNARE complexes and generated TeTx-sensitive monomeric SNAREs. However, compared with sperm from control WT mice, *ob*/*ob* mouse sperm had a significantly lower level of VAMP2 after progesterone stimulation, suggesting the faster disruption of *cis*-SNARE complexes and the poorer production of *trans*-SNAREs in *ob/ob* mouse sperm. The levels of TeTx-resistant VAMP2 in *ob*/*ob* mouse sperm was increased by the PTP1B inhibitor, suggesting that overdisruption of SNARE complexes in *ob/ob* mouse sperm is probably due to the sustained high activity of PTP1B.

The dynamic processes of *cis*-SNARE complex disassembly and the reassembly of *trans*-SNARE complexes during sperm acrosomal exocytosis are shown in Fig. 3*A*. To test the disassembly and reassembly process of SNARE complexes, we next used immunofluorescence and confocal microscopy to examine the localization patterns of two components of SNARE complexes, VAMP2 and SNAP25, in mouse sperm with or without progesterone stimulation. Because TeTx can cleave VAMP2 at the same peptide bond, but not SNAP25 (31), we used VAMP2 and SNAP25 as TeTx-sensitive and TeTx-resistant marker proteins of monomeric SNAREs, respectively. Sperm was fixed and double-labeled with mouse monoclonal anti-SNAP25 and rabbit polyclonal anti-VAMP2 antibodies. Under control conditions (without TeTx), clear immunofluorescence staining was observed in the acrosomal region of most cells (Fig. 3*B*). As expected, TeTx decreased the immunofluorescence labeling of the acrosome with the anti-VAMP2 antibody in sperm from both WT and *ob*/*ob* mice after progesterone was introduced, suggesting that progesterone induced the disassembly of *cis*-SNARE complexes, and VAMP2 became toxin-sensitive, whereas SNAP25 did not. However, compared with WT mice, *ob*/*ob* mice displayed almost no labeling of the

acrosome by anti-VAMP2 antibody, indicating that *cis*-SNARE complexes in *ob/ob* mice are faster and more completely disassembled under this condition. Because the labeling of the acrosome by anti-VAMP2 antibody was largely reversed following PTP1B inhibitor treatment, the sustained high PTP1B activity might be responsible for the disassembly of SNARE complexes via NSF dephosphorylation.

Abnormal PTP1B Activity-caused Defect of Sperm AR and Potential Therapeutic Effect of Specific PTP1B Inhibitor on Male Subfertility/Infertility—To test whether PTP1B has a similar effect on the AR of human sperm, we recruited a homogeneous group of 28 obese or overweight (body mass index >25) men with various degrees of subfertility/infertility and another group of 28 age-matched healthy donors. As shown in Fig. 4, *A* and *B*, PTP1B protein levels in the overweight and obese group was nearly 3-fold higher than those in the healthy group. Supporting this observation, we also detected significantly higher PTP1B activity in the overweight and obese group (Fig. 4*C*). PTP1B activity in the overweight and obese group was dose-dependently inhibited by the PTP1B inhibitor with a maximum inhibition at ~10 μM (Fig. 4*C*). Following a swim-up protocol to isolate highly motile cells, human semen samples were incubated in HTF medium, and the same steps of sperm acrosomal exocytosis were repeated. As shown in Fig. 4*D*, sperm from the obese or overweight group displayed a significantly less progesterone-induced AR compared with the sperm from the healthy group. The AR analysis by CTC staining showed that the sperm AR rate in the obese or overweight group was ~20% that of the healthy group, whereas the treatment with PTP1B inhibitor could significantly increase the AR rate of sperm from individual donors in the obese or overweight group (Fig. 4*E*).

DISCUSSION

By analyzing the level and activity of PTP1B in sperm and its effect on the sperm AR under various pathophysiological conditions, we demonstrated that PTP1B might serve as a key molecule in linking obesity and male infertility/subfertility. According to the model of sperm acrosomal exocytosis (Fig. 3*A*), successful AR requires the disassembly of *cis*-SNARE complexes and the reassembly of stable *trans*-SNARE complexes. Dephosphorylation of NSF by PTP1B is a key step in initiating the disassembly of *cis*-SNARE complexes. However, sustained high PTP1B activity in *ob*/*ob* mouse sperm would cause the suppression of the protein tyrosine phosphorylation events that are needed for exocytosis and would consequently halt the sperm AR. Interestingly, although the activity and expression of PTP1B were increased in *ob*/*ob* mouse sperm, the levels of tyrosine-phosphorylated NSF were not down-regulated in *ob/ob* mouse sperm (at resting status). We found that it was due to different location of PTP1B and phosphorylated NSF in the sperm (Fig. 2*A*). In particular, PTP1B was detected in the cytosol of the equatorial segment in capacitated mouse spermatozoa (7), whereas NSF was present in membranes of spermatozoa and localizes to the acrosomal region (33). Therefore, PTP1B inhibitor had no effect on phosphorylation of NSF in the absence of progesterone (Fig. 2*B*). Progesterone triggers the tethering of the acrosome to the plasma membrane, which initiates the activation and recruitment of PTP1B to the membrane fusion sites (6). After progesterone stimulation, PTP1B and NSF are co-localized in the acrosomal region. In addition, α-SNAP, an adaptor protein that mediates the binding of NSF to SNARE complexes, has been proved to be mainly in the cytosol of capacitated mouse spermatozoa (34), which control the initiation of AR before progesterone treatment. Taken together, AR is a tightly regulated process by segmentation of multiple key proteins to avoid spontaneous reaction.

In particular, sustained high PTP1B activity resulted in a prolonged dephosphorylation of NSF, a key regulator of vesicle fusion, leading to a defect of the reassembly of stable *trans*-SNARE complexes, which is the final step of sperm acrosomal exocytosis. Because the sperm from male *ob*/*ob* mice and obese or overweight men all contain significantly higher PTP1B level and activity than control mouse sperm and healthy human sperm, they generally displayed a significantly lower AR capacity. In support of this finding, we observed that a PTP1B-specific inhibitor could largely restore the AR capacity in the sperm from male *ob*/*ob* mice and obese or overweight men. A previous study by Huynh *et al.* (35) using lymphocytes shows that NSF is also a substrate for PTP-MEG2 (PTPN9) and can be dephosphorylated by PTP-MEG2. However, we found no significant difference between the levels of PTP-MEG2 in WT mouse sperm and *ob/ob* mouse sperm (data not shown), suggesting that PTP-MEG2 may be not contributed to the defect in AR of *ob*/*ob* mouse sperm. Previous studies have shown that PTP1B is a major negative regulator of insulin and leptin sensitivity by dephosphorylating the insulin receptor and the leptin receptor-associated JAK2 (13) as well as the more distal components of the insulin and leptin signaling pathways, such as insulin receptor substrate 1 (36, 37). PTP1B deficiency and the inhibition of PTP1B activity both enhance insulin signaling and insulin sensitivity in skeletal muscle and liver tissues (38–40). Our present study demonstrates that PTP1B is also a modulator of acrosomal exocytosis in the sperm. Through dephosphorylating NSF, PTP1B controls the disassembly and reassembly of SNARE complexes. Because a PTP1B inhibitor can restore the defect in sperm acrosomal exocytosis in both *ob*/*ob* mice and obese or overweight men, inhibition of PTP1B activity may provide a novel therapeutic strategy for obesity-associated male infertility or subfertility.

The *ob/ob* mice, with a loss of function mutation in the obesity (*ob*) gene, are generally infertile. The traditional view is that this infertility in *ob/ob* mice is due to low sex steroid and gonadotrophin levels. However, identification of sustained high PTP1B activity in *ob/ob* mice, which blocks the AR of sperm, provides a new clue that partially explains male infertility in *ob/ob* mice. Recent studies have also demonstrated that PTP1B is not only expressed in immune cells (41–43) but also up-regulated by proinflammatory factors, such as tumor necrosis factor α (TNFα) (44). Because obesity is considered a low degree inflammatory state characterized by an elevation of certain proinflammatory cytokines, including TNFα, interleukin-1, and interleukin-6 in sera (44), PTP1B may serve as an inflammatory target during obesity-associated inflammation (25, 32). By illustrating the correlation between the high expression level and activity of PTP1B and impaired acrosomal exocytosis in sperm under conditions of obesity, our present study may also provide

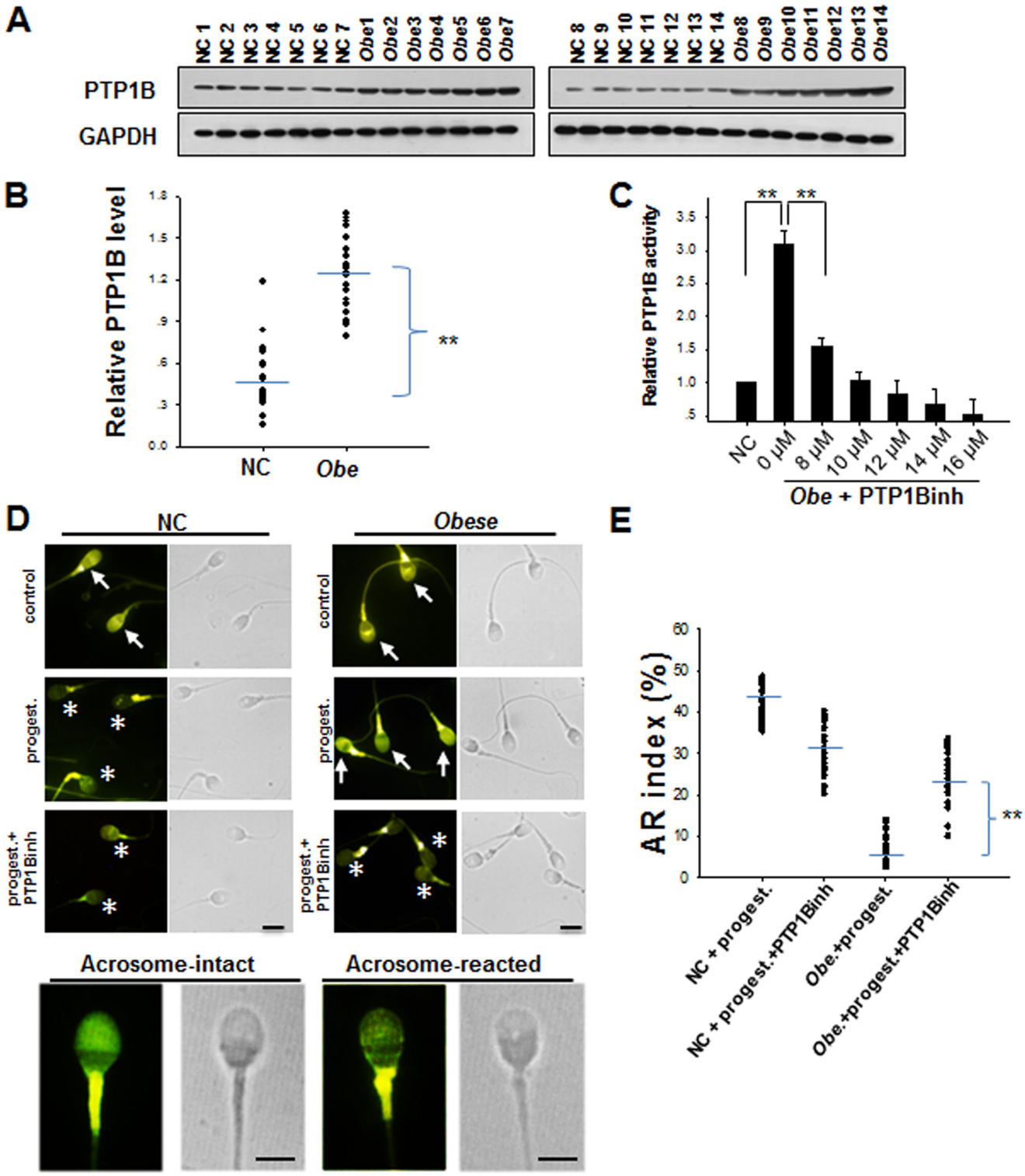

FIGURE 4. **The sperm from overweight or obese men have a sustained higher level of PTP1B expression and activity compared with the sperm from non-obese normal donors.** *A*, PTP1B protein levels in spermatozoa of 14 healthy non-obese men (*NC*) and 14 overweight or obese men (*Obe*). *B*, quantitative analysis of PTP1B levels in the sperm samples from 28 healthy men and 28 overweight or obese men. *C*, dose-dependent inhibition of PTP1B activity in spermatozoa from obese men. **, $p < 0.01$, $n = 7$. *D*, the AR of normal sperm (*NC*) and obese sperm (*Obe*) detected by CTC staining. All procedures were carried out in the dark until observation. By CTC staining, two different patterns of sperm were detected on the sperm head: acrosome-intact sperm (*arrows*) and acrosome-reacted sperm (*asterisks*). All sperm present strong labeling in the principal piece of the flagellum. *Scale bar*, 3 μm. *E*, quantitative analysis of CTC staining in *D*. A total of 200 spermatozoa from 28 non-obese and 28 obese donors were divided into the two above patterns to be analyzed. *Error bars*, S.D.

new insight to explain the correlation between chronic inflammation and infertility or subfertility. Specifically, our results indicate that PTP1B is a key molecule in linking chronic, "low degree" inflammation and male infertility. In this model, chronic inflammation, through TNFα or other proinflammatory factors, enhances the expression level and activity of

PTP1B, which consequently impairs the acrosomal exocytosis of sperm.

Acknowledgment—We thank Ruomeng Yang for technical support.

REFERENCES

1. Reis, L. O., and Dias, F. G. (2012) Male fertility, obesity, and bariatric surgery. *Reprod. Sci.* **19,** 778–785
2. Hammoud, A. O., Gibson, M., Peterson, C. M., Meikle, A. W., and Carrell, D. T. (2008) Impact of male obesity on infertility. A critical review of the current literature. *Fertil. Steril.* **90,** 897–904
3. Burgoyne, R. D., and Morgan, A. (2003) Secretory granule exocytosis. *Physiol. Rev.* **83,** 581–632
4. De Blas, G. A., Roggero, C. M., Tomes, C. N., and Mayorga, L. S. (2005) Dynamics of SNARE assembly and disassembly during sperm acrosomal exocytosis. *PLoS Biol.* **3,** e323
5. Rodríguez, F., Bustos, M. A., Zanetti, M. N., Ruete, M. C., Mayorga, L. S., and Tomes, C. N. (2011) α-SNAP prevents docking of the acrosome during sperm exocytosis because it sequesters monomeric syntaxin. *PLoS One* **6,** e21925
6. Zarelli, V. E., Ruete, M. C., Roggero, C. M., Mayorga, L. S., and Tomes, C. N. (2009) PTP1B Dephosphorylates *N*-ethylmaleimide-sensitive factor and elicits SNARE complex disassembly during human sperm exocytosis. *J. Biol. Chem.* **284,** 10491–10503
7. Tomes, C. N., Roggero, C. M., De Blas, G., Saling, P. M., and Mayorga, L. S. (2004) Requirement of protein tyrosine kinase and phosphatase activities for human sperm exocytosis. *Dev. Biol.* **265,** 399–415
8. Söllner, T. H. (2003) Regulated exocytosis and SNARE function (Review). *Mol. Membr. Biol.* **20,** 209–220
9. Roggero, C. M., De Blas, G. A., Dai, H., Tomes, C. N., Rizo, J., and Mayorga, L. S. (2007) Complexin/synaptotagmin interplay controls acrosomal exocytosis. *J. Biol. Chem.* **282,** 26335–26343
10. Tonks, N. K. (2006) Protein tyrosine phosphatases. From genes, to function, to disease. *Nat. Rev. Mol. Cell Biol.* **7,** 833–846
11. Tonks, N. K., and Neel, B. G. (2001) Combinatorial control of the specificity of protein tyrosine phosphatases. *Curr. Opin. Cell Biol.* **13,** 182–195
12. Dubé, N., and Tremblay, M. L. (2005) Involvement of the small protein tyrosine phosphatases TC-PTP and PTP1B in signal transduction and diseases: from diabetes, obesity to cell cycle, and cancer. *Biochim. Biophys. Acta* **1754,** 108–117
13. Bourdeau, A., Dubé, N., and Tremblay, M. L. (2005) Cytoplasmic protein tyrosine phosphatases, regulation and function: the roles of PTP1B and TC-PTP. *Curr. Opin. Cell Biol.* **17,** 203–209
14. Prada, P. O., Zecchin, H. G., Gasparetti, A. L., Torsoni, M. A., Ueno, M., Hirata, A. E., Corezola do Amaral, M. E., Höer, N. F., Boschero, A. C., and Saad, M. J. (2005) Western diet modulates insulin signaling, c-Jun N-terminal kinase activity, and insulin receptor substrate-1 Ser^{307} phosphorylation in a tissue-specific fashion. *Endocrinology* **146,** 1576–1587
15. Goldstein, B. J. (2002) Protein-tyrosine phosphatases: emerging targets for therapeutic intervention in type 2 diabetes and related states of insulin resistance. *J. Clin. Endocrinol. Metab.* **87,** 2474–2480
16. Shi, Q. X., and Roldan, E. R. (1995) Evidence that a GABAA-like receptor is involved in progesterone-induced acrosomal exocytosis in mouse spermatozoa. *Biol. Reprod.* **52,** 373–381
17. Lee, M. A., Trucco, G. S., Bechtol, K. B., Wummer, N., Kopf, G. S., Blasco, L., and Storey, B. T. (1987) Capacitation and acrosome reactions in human-spermatozoa monitored by a chlortetracycline fluorescence assay. *Fertil. Steril.* **48,** 649–658
18. Dadke, S. S., Li, H. C., Kusari, A. B., Begum, N., and Kusari, J. (2000) Elevated expression and activity of protein-tyrosine phosphatase 1B in skeletal muscle of insulin-resistant type II diabetic Goto-Kakizaki rats. *Biochem. Biophys. Res. Commun.* **274,** 583–589
19. Wu, Y., Ouyang, J. P., Wu, K., Wang, S. S., Wen, C. Y., and Xia, Z. Y. (2005) Rosiglitazone ameliorates abnormal expression and activity of protein tyrosine phosphatase 1B in the skeletal muscle of fat-fed, streptozotocin-treated diabetic rats. *Br. J. Pharmacol.* **146,** 234–243
20. Lam, N. T., Covey, S. D., Lewis, J. T., Oosman, S., Webber, T., Hsu, E. C., Cheung, A. T., and Kieffer, T. J. (2006) Leptin resistance following overexpression of protein tyrosine phosphatase 1B in liver. *J. Mol. Endocrinol.* **36,** 163–174
21. Ahmad, F., Azevedo, J. L., Cortright, R., Dohm, G. L., and Goldstein, B. J. (1997) Alterations in skeletal muscle protein-tyrosine phosphatase activity and expression in insulin-resistant human obesity and diabetes. *J. Clin. Invest.* **100,** 449–458
22. Cheung, A., Kusari, J., Jansen, D., Bandyopadhyay, D., Kusari, A., and Bryer-Ash, M. (1999) Marked impairment of protein tyrosine phosphatase 1B activity in adipose tissue of obese subjects with and without type 2 diabetes mellitus. *J. Lab. Clin. Med.* **134,** 115–123
23. Taghibiglou, C., Rashid-Kolvear, F., Van Iderstine, S. C., Le-Tien, H., Fantus, I. G., Lewis, G. F., and Adeli, K. (2002) Hepatic very low density lipoprotein-ApoB overproduction is associated with attenuated hepatic insulin signaling and overexpression of protein-tyrosine phosphatase 1B in a fructose-fed hamster model of insulin resistance. *J. Biol. Chem.* **277,** 793–803
24. Gum, R. J., Gaede, L. L., Koterski, S. L., Heindel, M., Clampit, J. E., Zinker, B. A., Trevillyan, J. M., Ulrich, R. G., Jirousek, M. R., and Rondinone, C. M. (2003) Reduction of protein tyrosine phosphatase 1B increases insulin-dependent signaling in ob/ob mice. *Diabetes* **52,** 21–28
25. Zabolotny, J. M., Kim, Y. B., Welsh, L. A., Kershaw, E. E., Neel, B. G., and Kahn, B. B. (2008) Protein-tyrosine phosphatase 1B expression is induced by inflammation *in vivo*. *J. Biol. Chem.* **283,** 14230–14241
26. Zinker, B. A., Rondinone, C. M., Trevillyan, J. M., Gum, R. J., Clampit, J. E., Waring, J. F., Xie, N., Wilcox, D., Jacobson, P., Frost, L., Kroeger, P. E., Reilly, R. M., Koterski, S., Opgenorth, T. J., Ulrich, R. G., Crosby, S., Butler, M., Murray, S. F., McKay, R. A., Bhanot, S., Monia, B. P., and Jirousek, M. R. (2002) PTP1B antisense oligonucleotide lowers PTP1B protein, normalizes blood glucose, and improves insulin sensitivity in diabetic mice. *Proc. Natl. Acad. Sci. U.S.A.* **99,** 11357–11362
27. Wiesmann, C., Barr, K. J., Kung, J., Zhu, J., Erlanson, D. A., Shen, W., Fahr, B. J., Zhong, M., Taylor, L., Randal, M., McDowell, R. S., and Hansen, S. K. (2004) Allosteric inhibition of protein tyrosine phosphatase 1B. *Nat. Struct. Mol. Biol.* **11,** 730–737
28. Xu, T., Rammner, B., Margittai, M., Artalejo, A. R., Neher, E., and Jahn, R. (1999) Inhibition of SNARE complex assembly differentially affects kinetic components of exocytosis. *Cell* **99,** 713–722
29. Sørensen, J. B., Wiederhold, K., Müller, E. M., Milosevic, I., Nagy, G., de Groot, B. L., Grubmüller, H., and Fasshauer, D. (2006) Sequential N- to C-terminal SNARE complex assembly drives priming and fusion of secretory vesicles. *EMBO J.* **25,** 955–966
30. Giraudo, C. G., Eng, W. S., Melia, T. J., and Rothman, J. E. (2006) A clamping mechanism involved in SNARE-dependent exocytosis. *Science* **313,** 676–680
31. Hayashi, T., McMahon, H., Yamasaki, S., Binz, T., Hata, Y., Südhof, T. C., and Niemann, H. (1994) Synaptic vesicle membrane fusion complex. Action of clostridial neurotoxins on assembly. *EMBO J.* **13,** 5051–5061
32. Xu, H., Barnes, G. T., Yang, Q., Tan, G., Yang, D., Chou, C. J., Sole, J., Nichols, A., Ross, J. S., Tartaglia, L. A., and Chen, H. (2003) Chronic inflammation in fat plays a crucial role in the development of obesity-related insulin resistance. *J. Clin. Invest.* **112,** 1821–1830
33. Michaut, M., Tomes, C. N., De Blas, G., Yunes, R., and Mayorga, L. S. (2000) Calcium-triggered acrosomal exocytosis in human spermatozoa requires the coordinated activation of Rab3A and *N*-ethylmaleimide-sensitive factor. *Proc. Natl. Acad. Sci. U.S.A.* **97,** 9996–10001
34. Tomes, C. N., De Blas, G. A., Michaut, M. A., Farré, E. V., Cherhitin, O., Visconti, P. E., and Mayorga, L. S. (2005) α-SNAP and NSF are required in a priming step during the human sperm acrosome reaction. *Mol. Hum. Reprod.* **11,** 43–51
35. Huynh, H., Bottini, N., Williams, S., Cherepanov, V., Musumeci, L., Saito, K., Bruckner, S., Vachon, E., Wang, X., Kruger, J., Chow, C. W., Pellecchia, M., Monosov, E., Greer, P. A., Trimble, W., Downey, G. P., and Mustelin, T. (2004) Control of vesicle fusion by a tyrosine phosphatase. *Nat. Cell Biol.* **6,** 831–839
36. Calera, M. R., Vallega, G., and Pilch, P. F. (2000) Dynamics of protein-tyrosine phosphatases in rat adipocytes. *J. Biol. Chem.* **275,** 6308–6312

37. Goldstein, B. J., Bittner-Kowalczyk, A., White, M. F., and Harbeck, M. (2000) Tyrosine dephosphorylation and deactivation of insulin receptor substrate-1 by protein-tyrosine phosphatase 1B. Possible facilitation by the formation of a ternary complex with the Grb2 adaptor protein. *J. Biol. Chem.* **275,** 4283–4289
38. Klaman, L. D., Boss, O., Peroni, O. D., Kim, J. K., Martino, J. L., Zabolotny, J. M., Moghal, N., Lubkin, M., Kim, Y. B., Sharpe, A. H., Stricker-Krongrad, A., Shulman, G. I., Neel, B. G., and Kahn, B. B. (2000) Increased energy expenditure, decreased adiposity, and tissue-specific insulin sensitivity in protein-tyrosine phosphatase 1B-deficient mice. *Mol. Cell Biol.* **20,** 5479–5489
39. Bence, K. K., Delibegovic, M., Xue, B., Gorgun, C. Z., Hotamisligil, G. S., Neel, B. G., and Kahn, B. B. (2006) Neuronal PTP1B regulates body weight, adiposity and leptin action. *Nat. Med.* **12,** 917–924
40. Kahn, B. B., and Flier, J. S. (2000) Obesity and insulin resistance. *J. Clin. Invest.* **106,** 473–481
41. Simoncic, P. D., Bourdeau, A., Lee-Loy, A., Rohrschneider, L. R., Tremblay, M. L., Stanley, E. R., and McGlade, C. J. (2006) T-cell protein tyrosine phosphatase (Tcptp) is a negative regulator of colony-stimulating factor 1 signaling and macrophage differentiation. *Mol. Cell Biol.* **26,** 4149–4160
42. Simoncic, P. D., McGlade, C. J., and Tremblay, M. L. (2006) PTP1B and TC-PTP. Novel roles in immune-cell signaling. *Can. J. Physiol. Pharmacol.* **84,** 667–675
43. Heinonen, K. M., Bourdeau, A., Doody, K. M., and Tremblay, M. L. (2009) Protein tyrosine phosphatases PTP-1B and TC-PTP play nonredundant roles in macrophage development and IFN-γ signaling. *Proc. Natl. Acad. Sci. U.S.A.* **106,** 9368–9372
44. Iacobellis, G., and Barbaro, G. (2008) The double role of epicardial adipose tissue as pro- and anti-inflammatory organ. *Horm. Metab. Res.* **40,** 442–445